Analysis of #2 Winthrop Williams' CR-39 detector after SPAWAR/Galileo type electrolysis experiment

Andrei Lipson[1], Alexei Roussetski[2], Eugeny Saunin[1]
[1]Institute of Physical Chemistry and Electrochemistry, Russian Academy of Sciences, Moscow 119991, Russia
[2]P.N. Lebedev Physics Institute of RAS, Moscow 119991, Russia

1. Introduction

The experimental goal of this work was to search for reality of nuclear tracks in SPAWAR/Galileo type experiment described by W. Williams in his APS March 2007 Meeting presentation. [1]

The experimental conditions of SPAWAR experiments are as follows. Electrolysis was carried out in solution 0.03 M $PdCl_2$ + 0.3 M LiCl in D_2O. The anode was a platinum wire (0.25 mm in diameter); the cathode was a palladium wire (0.25 mm in diameter). A CR-39 detector (Landauer 1 × 2 cm^2) was attached to the cathode wire during electrolysis. Then it was etched in 6.5 NaOH for 3 h at 68°C.

2. Calibrations

From April to May 2007 we performed a manual analysis of Williams' #2 CR-39 detector which had been subjected to a Galileo/SPAWAR type of electrolysis experiment at the University of California at Berkeley (UCB). The detector was attached to the wire cathode (without using a Mylar filter) during the Pd deposition experiment in deuterium electrolyte. After electrolysis, Williams etched the detector in NaOH solution. In order to estimate the etching conditions in UCB we have been supplied by Williams' calibration detector irradiated with an Am-241 alpha source (E_α = 5.45 MeV) and etched in the same condition as the #2 detector.

In our first step we determined the track diameter of Williams' calibration detector and found that it is underetched compared with our standard conditions of minimal required etch (6 N NaOH at T = 70°C, t = 7 hr) which is a starting point for our calibration curves. To achieve this goal we performed an additional etch in our standard conditions for 1 hr 45 min and then compared the obtained track diameters with our calibrations (Fig. 1).

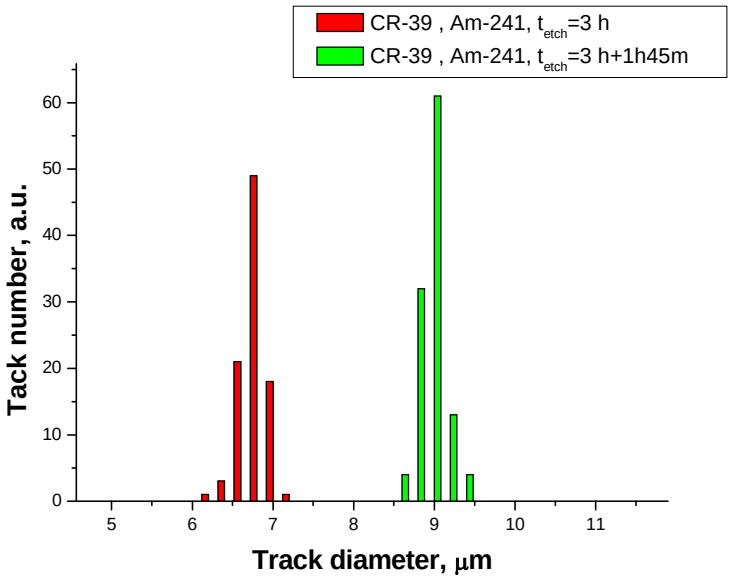

Figure 1. Estimation of etching condition of Williams' calibration detector irradiated with Am-241 alpha source (E_α = 5.45 MeV).

It was found that under Williams' etching conditions the mean track diameter for 5.45 alphas is 6.7 μm. In order to move to our standard condition (see Figure 2) we carried out an additional etch of this detector for 1 hr 45 min. After this additional etch the track diameter for Am-242 alphas was increased to 8.9 μm, which is within the measurement error, and is in satisfactorily agreement with out calibration data (at E_α = 5.45 MeV it should be ~8.7 μm). Taking into account this result, the Williams' Foreground detector #2 was additionally etched in 6 N NaOH at 70°C for 1.5 hr.

In the first approximation, the track diameters obtained after Williams' etching plus our additional etching for 1 hr 45 min are quite similar to track diameters from our 7 hr etching conditions. To check the validity of this we preformed an etch of Williams' alpha-detector for additional 7, 14 and 21 hr and compared the results with our Landauer calibration curves for alpha particles with energies of 5.15 and 6.0 MeV. The result is shown below and gives perfect agreement with our alpha curves (Fig. 2).

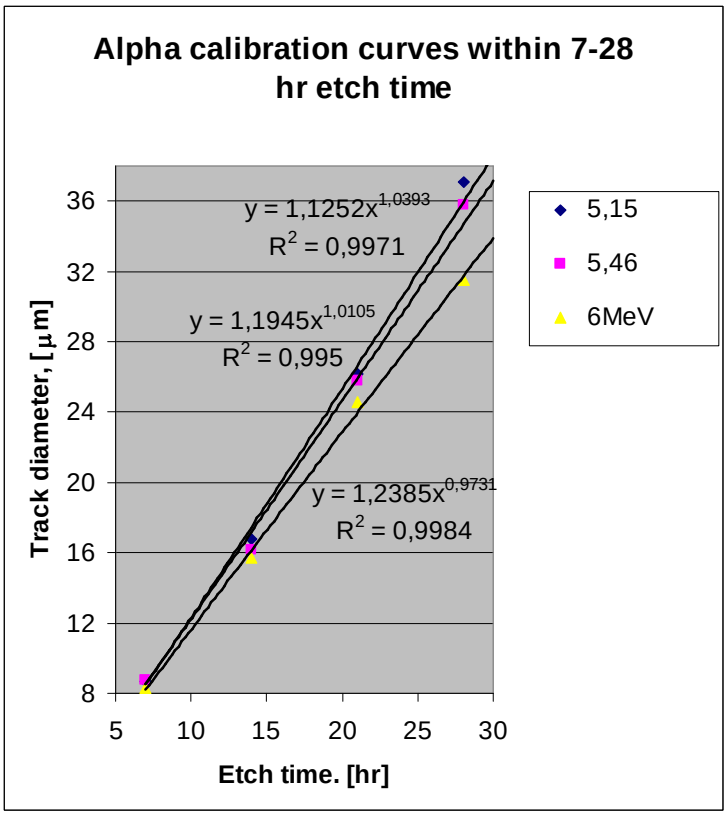

Figure 2. Comparison of Williams' alpha track (5.46 MeV) distribution vs. etch time (D(t)) with our 5.15 and 6.0 MeV D-t curves. As seen all curves are well fitted by power functions: the 5.46 MeV (Williams') curve is located between 5.15 and 6.0 D(t) curves. This figure confirms that the additional etch during 1.5 hr in 6 N NaOH at T = 70°C provide the right conditions for further etch, enabling us to compare tracks/pits at Williams' #2 detector with our calibration D(t) curves.

Thus, for Williams' #2 detector analysis (starting at his 3 hr + our 1.5 hr etch) we will use our calibration curves.

Because the main goal of this analysis was to establish whether or not the pits at the surface of the #2 detector could be ascribed to nuclear tracks, we carried out a comparison of the Williams' pit images and D(t) functions with our calibrations for alphas and protons. Figures 3a and 3b show the calibration curves of track diameters D vs. alpha and proton energies for etch time within 7-28 hr in 6 N NaOH at T = 70°C (bulk etch rate v_b = 1.32 μm/hr) for alphas in the range of 2-12.8 MeV and protons of 0.5-3.0 MeV.

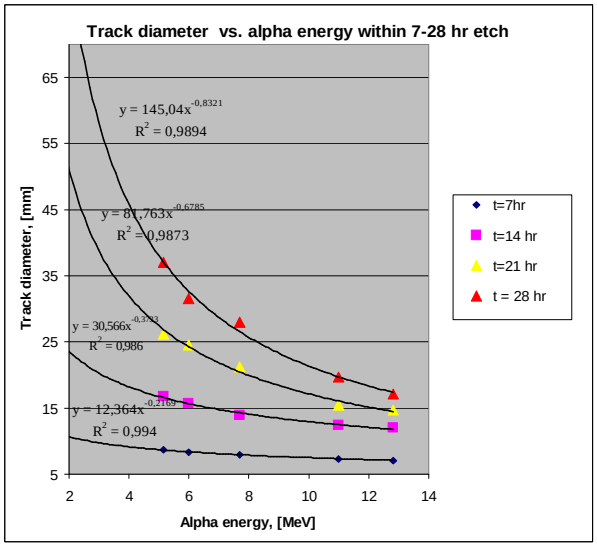

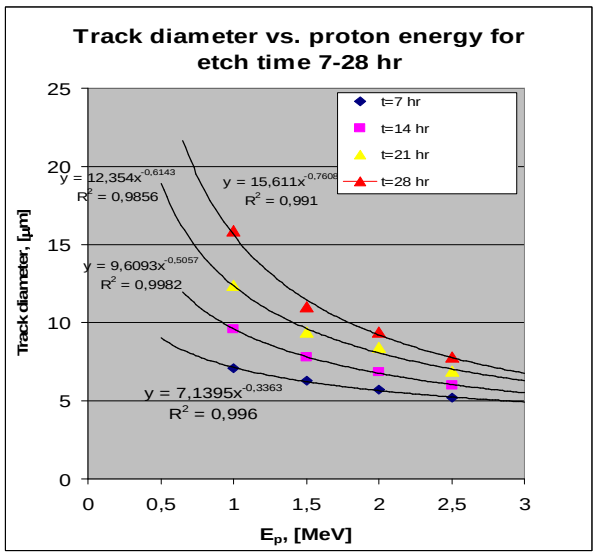

Figure 3 a, b Alpha (a) and proton (b) calibration curves (D vs. E) for etch time 7-28 hr.

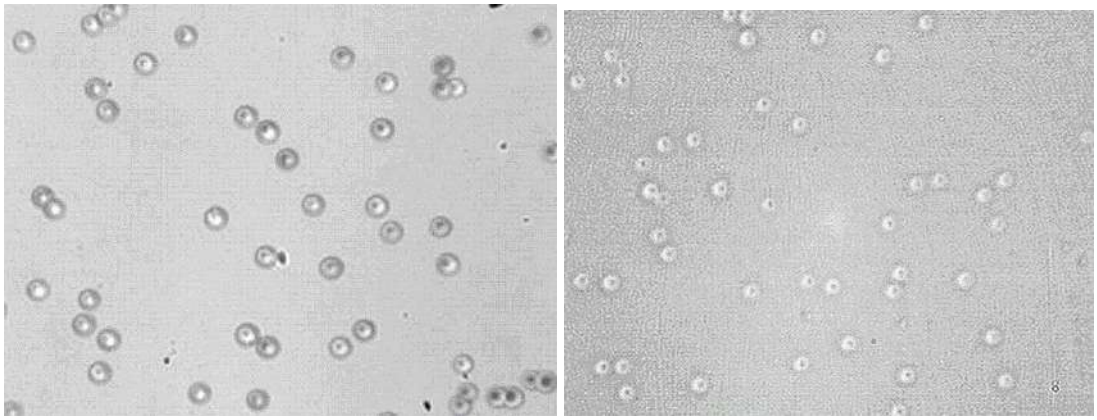

a) b)

Figure 4a. This is how real nuclear tracks look. Tracks from 11.0 MeV α-beam at normal incidence with respect to CR-39 (Landauer) target: image area S = 0.12 × 0.09 mm^2, (× 600). The track density is about 10^6 track/cm^2. The conic shape of alpha tracks is clearly visible as a small dark hole in the center of the pit.
Figure 4b. Proton tracks. Tracks from 2.5 MeV p-beam at normal incidence with respect to the CR-39 (Landauer) target: image area S = 0.12 × 0.09 mm, (× 600). The conic shape of proton tracks is also clearly seen as a small dark hole in the center of the pit (cavier effect).

3. #2 Detector Pit Analysis

The pit density at the etched scratch area produced by the contact of the cathode wire with the surface of CR-39 detector is very large (N > 10^8 pit/cm^2). In contrast, the back side of the #2 detector contains almost no pits. Most of the pits on the front side (which is attached to the cathode wire) are overlapped and cannot be analyzed properly in terms of their shape and diameter range. In order to provide such an analysis we have chosen only individual pits (that were not overlapped) in the area surrounding the scratch (total area S = 2.0 mm^2), and we carried out measurements of their diameters at etching time t = 7, 14 and 21 hr (Figs. 5-7).

The total CR-39 etching must be similar to our standard conditions (Figs. 2, 3): 6 N NaOH, T = 70°C, for 7 hr. Notice that for correct determination of track diameter we cannot take overlapping pits. So, only individual pits were chosen. The pits are located in the wide range of the diameters within 1- 20 μm. All of them are placed mainly along the scratch that is visible at the surface of CR-39 as a trace of the attached electrode. No tracks were found at the back side (opposite to the surface where the electrode was attached) of this Foreground detector.

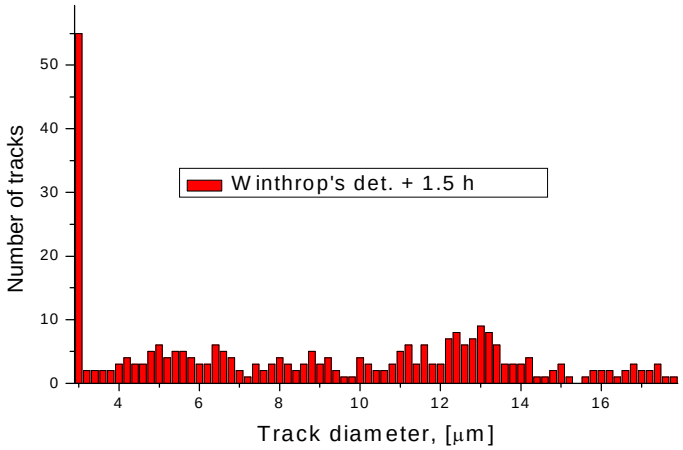

Figure 5. Individual track diameter distribution for Williams' Foreground detector after additional 1.5 hr etching in 6N NaOH solution at T =70°C (equivalent to our etch time t = 7 hr).

Note also that many pits (about a third) have a diameter d < 3 μm. In reality the peak at d = 3 μm in the graph corresponds to all pits with d < 3 μm. These pits cannot be ascribed to nuclear tracks because they would only be consistent with protons with E_p > 30 MeV with very low critical angle, suggesting negligibly small detection efficiency. The pits at d > 12 μm cannot be ascribed to alphas because the detected alphas have track diameter d ≤ 12 μm (see Fig. 3 a). No elliptically shaped pits were found, suggesting absence of particles with oblique incidence. (Yet, if the wire is the source of the pits, it would have to produce many pits with oblique incidence.) Moreover, 30 MeV protons can pass through the 0.85 mm thick CR-39 detector, assuming appearance of pits at the back side of this CR-39. The absence of tracks at the back side of the CR-39 also gives us a clue that no measurable neutron flux was emitted during this electrolysis run.

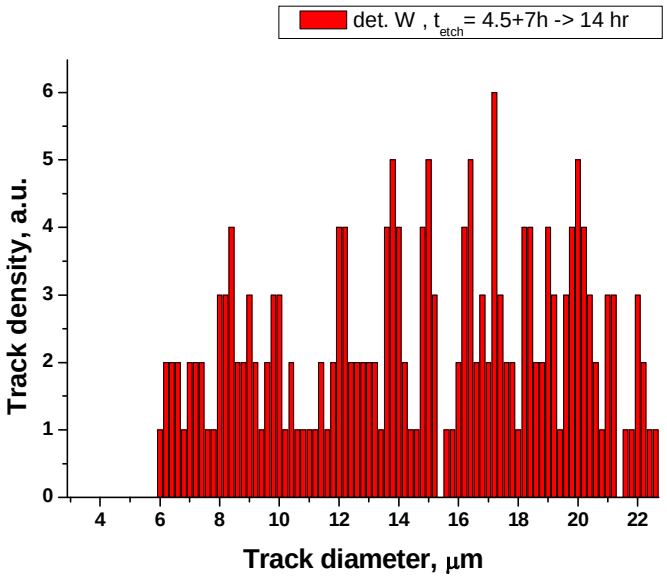

Figure 6. Individual track diameter distribution for Williams' Foreground detector #2 after additional 7 hr (4.5 hr + 7 hr → 14 hr) etch in 6 N NaOH solution at T = 70°C (equivalent to our etch time t = 14 hr). Notice a full disappearance of the small diameter pits with d < 6.0 μm. If pits with d < 3 μm were high energy proton tracks, their diameters would be almost unchanged (very small increase in d). The disappearance of small pits thus shows that they are small, shallow surface defects caused by mechanical stress at the CR-39 surface. These defects will overetch very quickly and their images lose contrast with etching in depth, and become invisible.

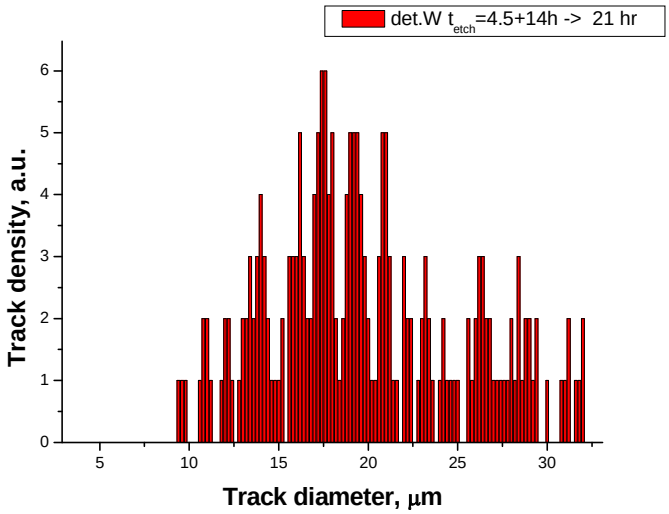

Figure 7. Individual track diameter distribution for Williams' Foreground detector #2 after additional 14 hr (4.5 hr + 14 hr → 21 hr) etch in 6 N NaOH solution at T =70°C (equivalent to our etch time t = 21 hr).

Notice the complete absence of tracks with d < 10 μm and d > 30 μm showing an absence of possible protons with energy E > 1.5 MeV and alphas (E < 4 MeV), respectively. No significant shift of pit diameter maximums (which could be ascribed to the effect of stopping power of CR-39 material) is seen compared to the 14 hr etch. (Compare maximum between 16-18 μm track range in 14 hr etched detector with that between 15 and 20 μm tracks in the 21 hr etched detector.)

Thus the analysis of pit diameter distributions on etching in depth show that majority of the pits in #2 CR-39 are surface defects and cannot be ascribed to nuclear tracks.

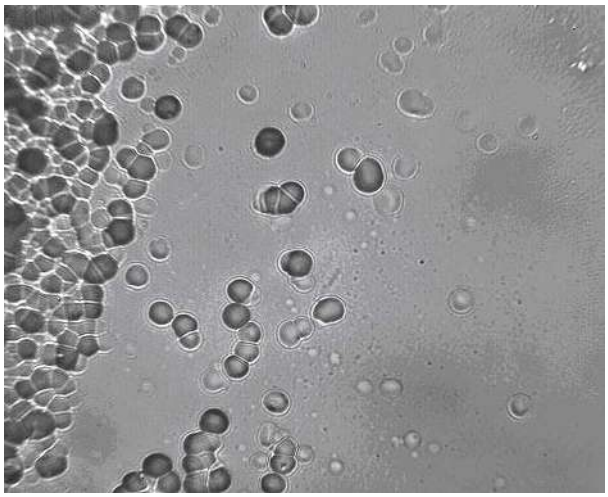

(a)

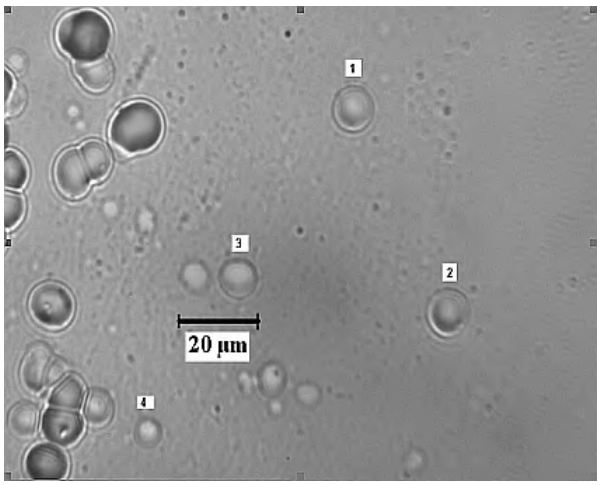

(b)

Figure 8. (a) The image of the front side of the #2 detector with the fixed coordinates [x,y] = [1028, 1075]. Etch time is t = 7 hr. (b) The same area at a higher magnification (×3). The individual selected pits 1-4 of the right shape (in terms of smoothness) with the size ranging from 5 to 12 μm are indicated.

4. Images of Williams' #2 detector and pits simulation

Figure 8 shows examples of pit agglomerations obtained from Williams' Foreground detector. (In CR-39 jargon we call such pit agglomerations "ground beef" and never take them into consideration.) All of these pits are located along the scratch produced by the wire electrode tightly attached to the front side of CR-39 detector chip. The conic shape of track required for nuclear track is not observed. Below the images of the front face of #2 detector containing also individual pits (separated by space one from another) are depicted. Our long experience shows that massive overlapped pits can be seen at the CR-39 surface after intensive mechanical deformation of the detector chip. We show these examples too in order to provide additional clues as to how at least some of the SPAWAR pits could have originated. In all cases presented (unless otherwise noted) the size of the image is equal to $280 \times 220\ \mu m^2$.

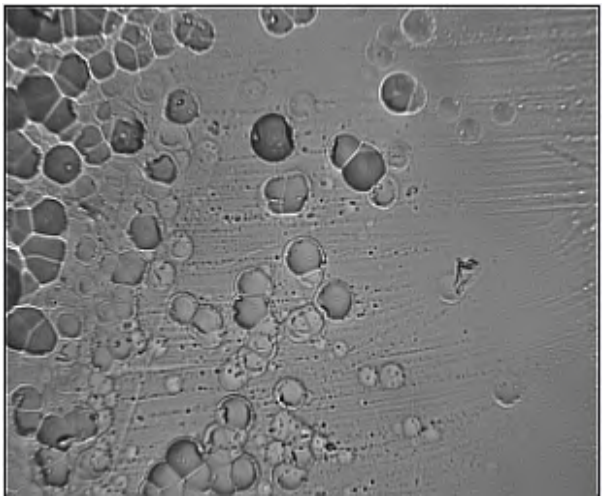

(a)

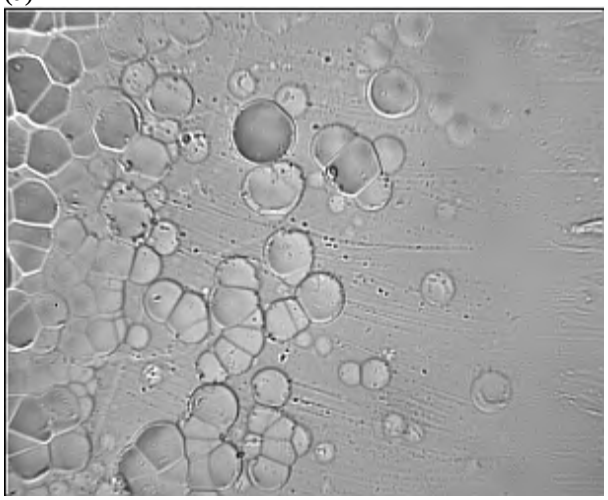

(b)

Figure 9 (a,b) – The same as in Fig. 8a image with the fixed coordinates[1028,1075] after total etch time during 14 hr (a) and 21 hr(b). Note to the deviation of the pit shape from the smoothness (circular or elliptic shape) with increase in etch time (the pits become of a sharp shape and partially loose a contrast). This is also indicates that these pits are not from nuclear particles because nuclear tracks are keeping their smooth shape.

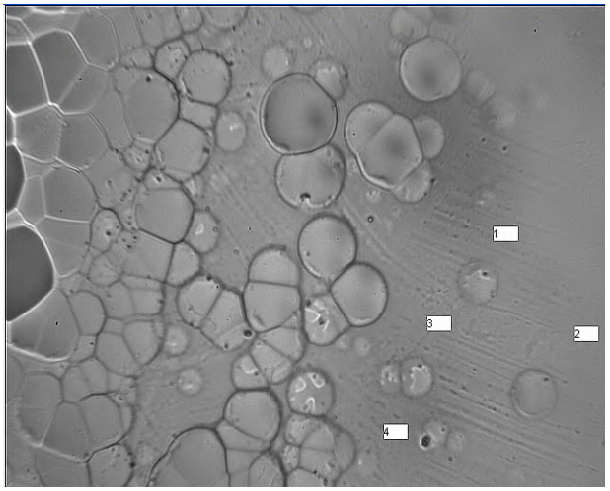

Fig. 10. The image of the front side of the #2 detector with the fixed coordinates [1028, 1075]; etch time is t =28 hr . The same individual pits 1-4 as indicated in Fig. 8 b are marked.

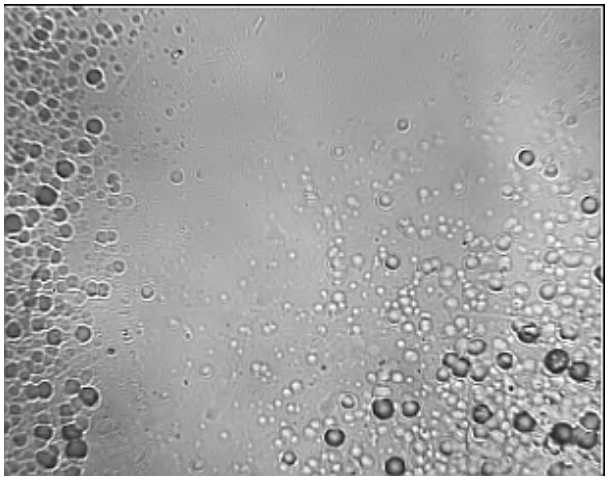

Figure 11. Another example of the #2 detector image containing a lot of small pits (d < 4 μm): the spot with the coordinates [663,435]. Etch time is equivalent to t=7 hr.

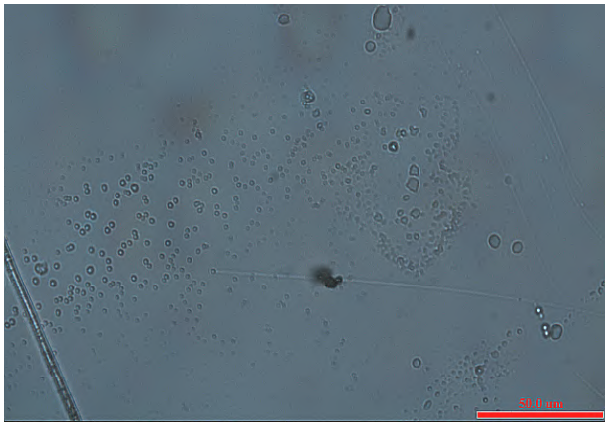

Figure 12. Track simulation with mechanical stress. The 200 μm Pt wire is attached tightly to the surface of the Landauer CR-39 detector (scratch in the left corner of the image) for 2 days before etching. Etch time is t = 7.0 hr. Lots of pits, mainly of small diameter (d < 4 μm) are appeared. Compare the size of small pits with that seen in [663,435] image of Williams' detector.

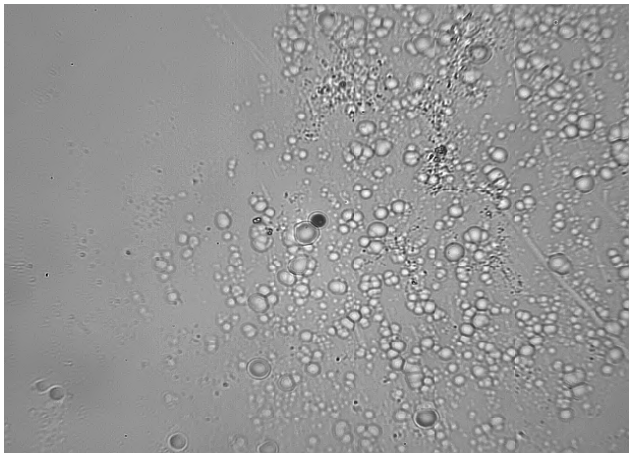

Figure 13. Another example of pits simulation by mechanical stress: the rough 50 micron thick Pd foil is pressed tightly to the surface of the Landauer CR-39 detector (no electrolysis) with a hard clamp for one week. Etch time t = 7 hr. The size of majority of pits is 3 – 10 μm. Dark pit in the center is a real alpha-particle track.

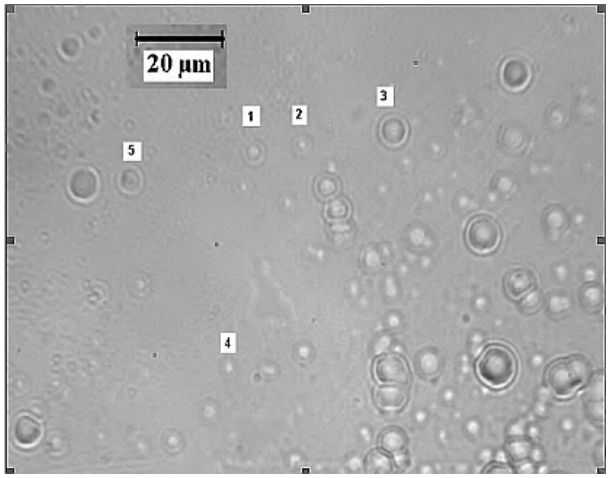

Figure 14. The image of the [663,435] spot. Etch time t = 7 hr. The same area as in Fig. 11 with the higher magnification (x3); the individual selected circular pits 1-5 of the right (in terms of smoothness) shape with the size ranging of 5-12 micron are indicated (b).

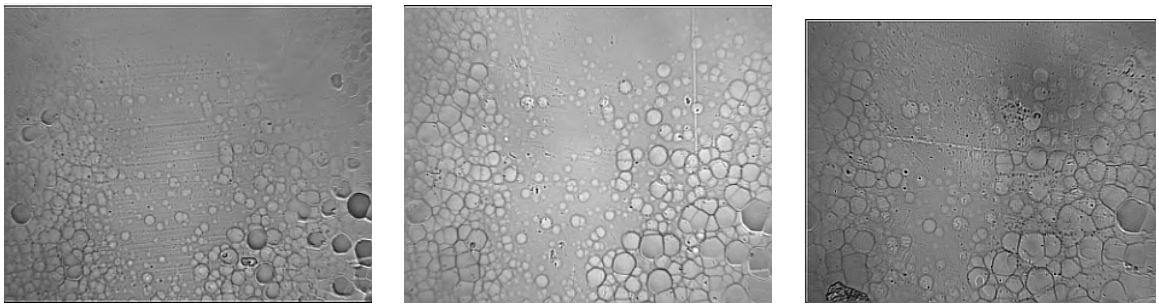

(a) (b) (c)

Figure 15 (a-c). The image of the [663,435] spot at etch time t = 14hr (a), 21 hr (b) and 28 hr (c), respectively. With increase of removed depth, majority of pits lose contrast and become of the sharp angle (noncircular) shape.

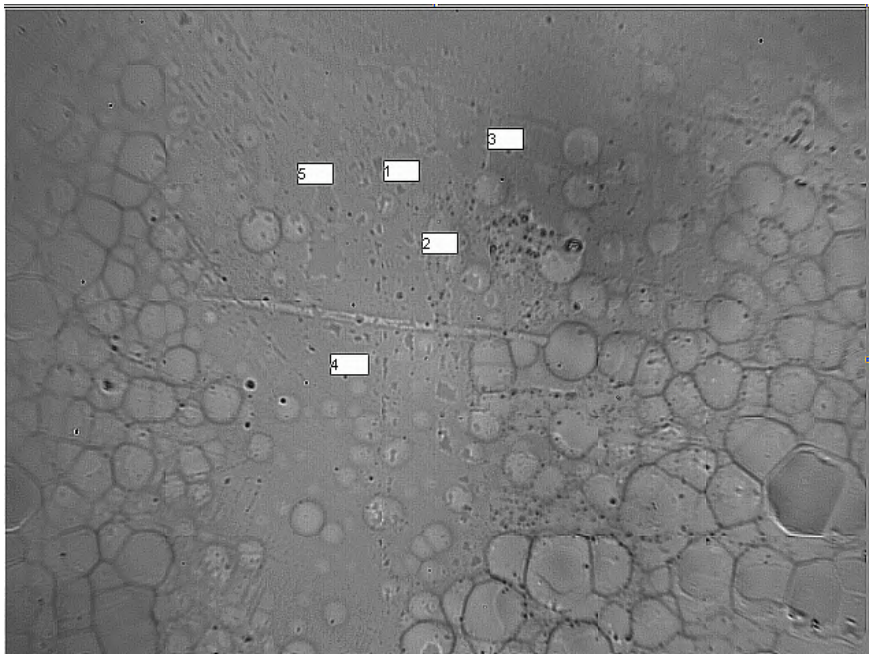

Figure 16. The same spot as in Fig. 15c, with selected pits 1-5 indicated.

5. Etch rate of individual selected pits: comparison with the alpha and proton track diameter growth rate

Below, we extract quantitative information on the origin of some pits selected in spots [1028, 1075] and [663,435]. We have to select pits of the right shape and size. The dynamics of etching, reflecting the track etch rate, allow us to unambiguously identify the type and energy of nuclear particles. To this aim, in the present report we can use the slope of the D(t) curve (where D is the track diameter, and t is the etch time), which effectively reflects the etch rate inside the track (v_t).

The etch rate in the track is determined by the function $v_t = \partial L/\partial t$ (where L is the track length). Noting that $L = D/2 \text{ tg } \delta$, where δ = const (at v_t = const) is the local developing angle of the track we obtain that $v_t = A\ (\partial D/\partial t)$, where A is a constant. Thus, the slope of track diameter function vs. etch time t would effectively reflect the etch rate of the pit. A similar procedure of track identification, involving the comparison of selected track dynamics with that of alphas and protons with appropriate track diameter, was already demonstrated in our previous work (see A.S. Roussetski *et al.*, Proc. ICCF-12, Japan, 2005).

To begin this procedure we take selected track with the measured initial diameter D corresponding to minimal removed detector depth (in our case at t = 7 hr) and we

compare its diameter growth with etching in depth to that of a nuclear particle with exactly the same initial diameter D as the selected track.

The graphs of the etching dynamics for each selected pit 1-4 from the [1028,1075] spot and for appropriate nuclear particles (with the same initial diameter at t = 7 hr) are presented below in Fig. 17 (a-c).

The graphs of the etching dynamics for each selected pit 1-5 from the [663,435] spot and for appropriate nuclear particles (with the same initial diameter at t = 7 hr) are presented below in Fig. 18 (a-c).

Thus all of the analyzed pits from both spots show the slope of dD/dt function that is a factor 2-10 smaller than corresponding alpha/proton tracks with the same initial diameter as for the selected pits. Moreover, the dD/dt function of the pits cannot be satisfactorily fitted by a power function (in most cases $R^2 < 0.98$), that normally describes charged particle diameter growth during etching in-depth. These findings unambiguously suggest that those selected pits have a lower etch rate (inside the "track") than the nuclear particles producing the tracks of the same initial diameter at t = 7 hr. Thus, these selected pits of the right shape and size consistent with the nuclear particle tracks cannot be ascribed to the tracks of nuclear particles.

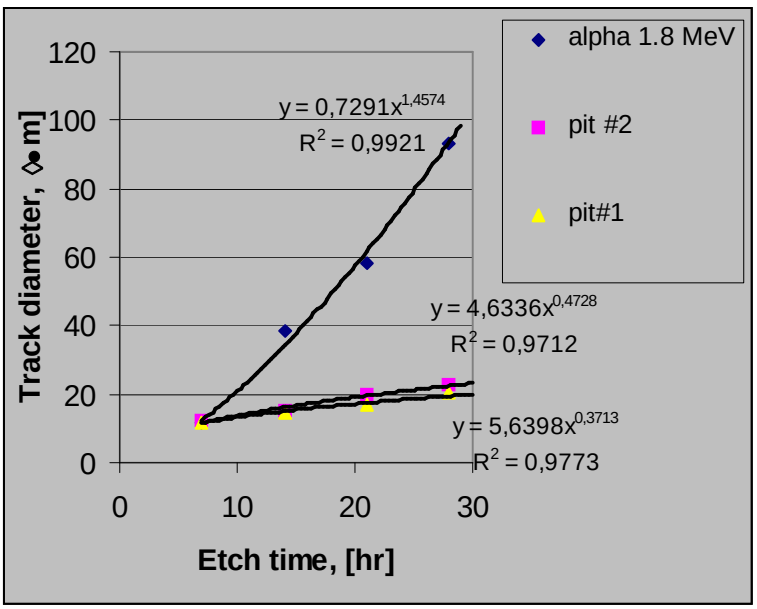

(a)

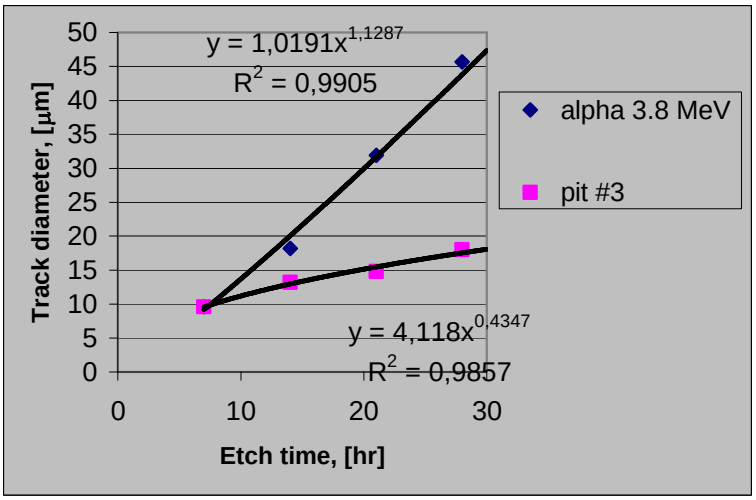

(b)

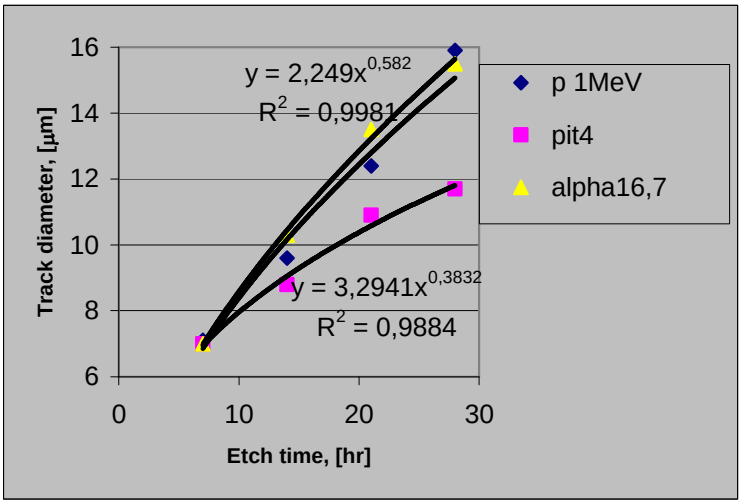

(c)

Figure 17 (a-c) Etch dynamics for pits 1-4 from the spot [1028,1075] as well as for appropriate nuclear particles (p-proton, a – alpha) of the same initial diameter. As seen, the slope of the pits 1-4 is about factor of 2 - 6 less than that for appropriate nuclear particles.

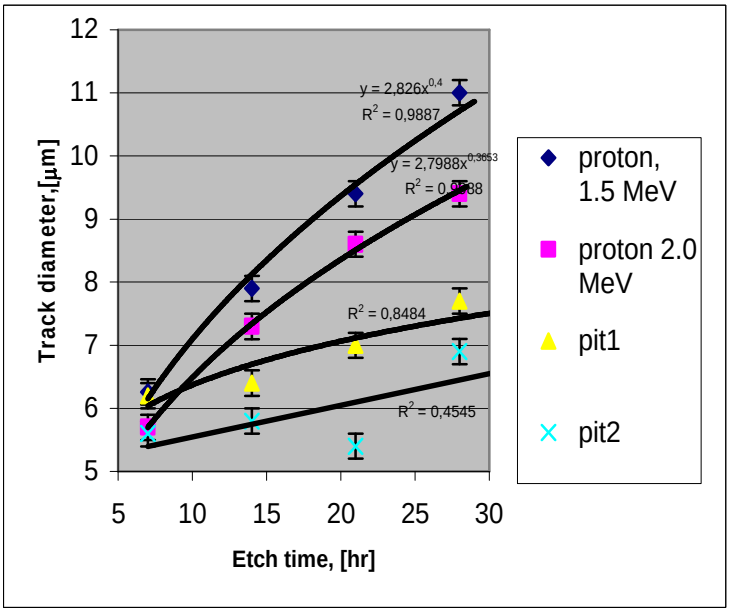
Track diameter,[µm]
Etch time, [hr]
y = 2,826x^0,4
R² = 0,9887
y = 2,7988x^0,3653
R² = 0,8484
R² = 0,4545
proton, 1.5 MeV
proton 2.0 MeV
pit1
pit2

(a)

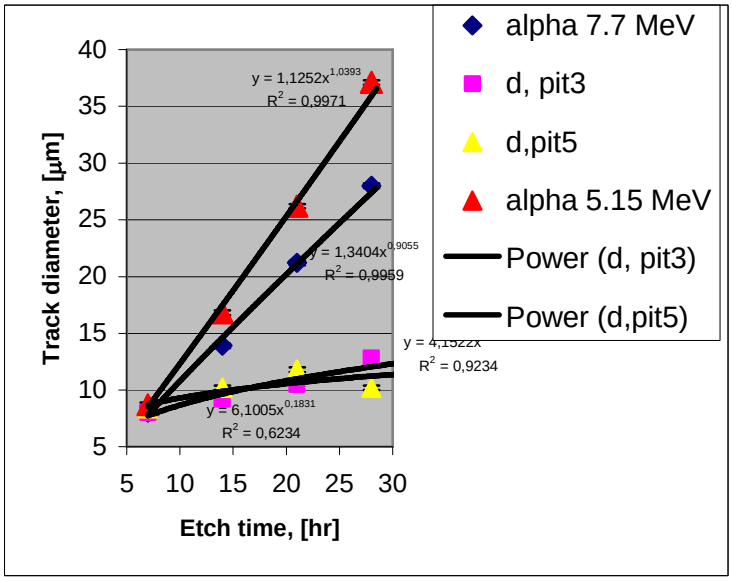
Track diameter, [µm]
Etch time, [hr]
y = 1,1252x^1,0393
R² = 0,9971
y = 1,3404x^0,9055
R² = 0,9959
y = 4,1522x
R² = 0,9234
y = 6,1005x^0,1831
R² = 0,6234
alpha 7.7 MeV
d, pit3
d,pit5
alpha 5.15 MeV
Power (d, pit3)
Power (d,pit5)

(b)

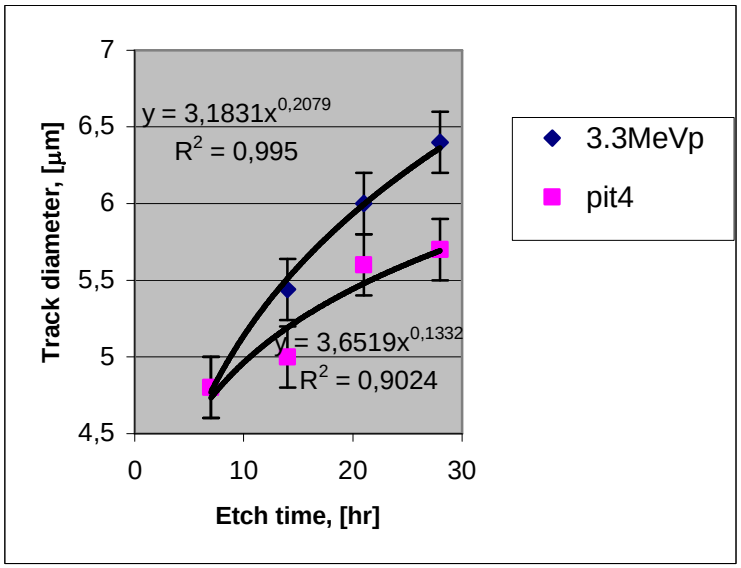

(c)

Figure 18. Etch dynamics for pits 1-5 from the spot [663,435] as well as for appropriate nuclear particles (p-protons, a – alphas) of the same initial diameter. As seen, the slope of the pits 1-5 is about factor of 2 - 10 smaller than that for appropriate nuclear particles.

6. Conclusions

The total dataset obtained during our analysis of the #2 Williams detector do not show any signature of real nuclear tracks. The main peculiarities of the observed pits force us to come to the following negative conclusions:

- High density overlapping pits near the scratch from the cathode wire. During the etching in depth these pits lose their smooth circular shape (which is a signature of nuclear particles), and they lose contrast. The last factor indicates that these pits are shallow.
- The individual analyzed pits show three groups of diameters: $D < 5$ μm, $D > 12$ μm and 5 μm $< D < 12$ μm at etch time equivalent to $t = 7$ hr. The first two groups, according to our calibrations, cannot be ascribed to proton and alpha particles. The group with $D < 5$ μm totally disappeared after 14 hr etching, indicating shallow surface defects. The group of pits with $D > 12$ μm also cannot be ascribed to heavy nuclear particles (Li^6 or heavier ions) because these pits demonstrate very slow dynamics of their diameter growths, which is contrary to what is expected for heavy ions.
- Almost no elliptically shaped pits were found among either the overlapping or individual tracks, suggesting the absence of the projectile particles with oblique incidence. This is not possible if the source of these particles is at the cathode

wire attached to the CR-39 surface. A source at this location would have to produce pits with oblique incidence.

- The group of pits with appropriate minimal diameter (5 μm < D < 12 μm) consistent with protons and alpha tracks at etch time t = 7 hr do not demonstrate the track etch rate required for those nuclear particles. The etch rate for these pits is 2-10 times lower, indicating that radiation destruction of CR-39 material inside the pits is significantly less than that from the nuclear particles.
- The similar high density pits of low and medium diameter range can be successfully simulated by mechanical stress. This generates a massive number of defects at the surface of the CR-39 detector with the attached wire. The application of magnetic/electric field to the detector would only enhance the mobility of charged defects and thereby intensify pit formation.

Acknowledgements

This work was supported by New Energy Institute. We also personally thank S. Krivit, E. Greenspan, and L. Forsley for arranging this work as well as for valuable discussions.

References

[1] Williams, “Search for Charged Particle Tracks Using CR-39 Detectors to Replicate the SPAWAR Pd/D External Field Co-Deposition Protocol” March 2007 APS Meeting, Denver, Co.

[2] A.G. Lipson *et al.*, Proc. ICCF-12, ed. A. Takahasi *et al.*, p. 293, World Scientific, 2006.